



Pergamon

Tetrahedron 56 (2000) 8833–8839

TETRAHEDRON

Confirmation and Characterization of the Hypervalent Sb···N Bonding Recognized in Triarylstibanes Bearing an Amino Side Chain by X-Ray, NMR and Theoretical Calculations

Tatsuhiko Tokunaga,^a Hiroko Seki,^a Syuji Yasuike,^b Masaaki Ikoma,^b Jyoji Kurita^{b,*} and Kentaro Yamaguchi^{a,*}

^aChemical Analysis Center, Chiba University, Inage-ku, 1-33 Yayoicho, Chiba 263-8522, Japan

^bFaculty of Pharmaceutical Sciences, Hokuriku University, Ho-3 Kanagawa-Machi, Kanazawa 920-1181, Japan

Received 24 July 2000; accepted 11 August 2000

Abstract—Hypervalent Sb···N bonding observed in triarylstibanes was investigated by single-crystal X-ray diffraction study, comparison of the ¹⁵N chemical shifts, and HMBC NMR spectroscopic detection of the ¹H–¹³C long-range coupling. This bonding is strongly dependent on the Lewis acidity of the central antimony atom. A good correlation was observed between ¹⁵N chemical shift and the charge distribution obtained from semi-empirical molecular orbital calculations. © 2000 Elsevier Science Ltd. All rights reserved.

Introduction

Recently, slight shortening of the interatomic distances in comparison with the sum of the van der Waals radii between group 14–16 elements and other heteroatoms such as oxygen or nitrogen has been found in certain compounds. This interaction, which is classified as hypervalent bonding, transcends the octet theory, and is of interest because of the effect it may have on the structure, chemical properties and biological activities.^{1–8} We have found, by means of X-ray analysis, that the interatomic distances between group 15 elements and oxygen or sulfur were 80–90% of the sum of the van der Waals radii in 1,6-diheteroethines (C₂₂H₁₇OSb), 10-membered ring compounds obtained by electrophilic ring closure of the corresponding 1,9-dilithium compounds.⁹ Most of the interactions involving group 15 elements were observed in compounds with a cyclic structure, suggesting the influence of steric factors.^{10–12} In this study, we have prepared various antimony(III, V) compounds bearing a phenyl and/or naphthyl substituent with –NMe₂ or –CH₂NMe₂ in the *ortho*-position in order to investigate the origin of the above interactions. These compounds having conformational flexibility of the nitrogen functionality were designed to be able to introduce Cl atoms in order to change the valence of Sb atom. Antimony was selected as the most suitable element in the group 15 in order to avoid the use of poisonous arsenic compounds or

unstable bismuth compounds. Here we described the confirmation and characterization of the hypervalent Sb···N bonding recognized in triarylstibanes (C₂₃H₁₆NSb) and their dichlorides, by means of X-ray crystallography, NMR spectroscopy and semi-empirical theoretical calculations.

Results and Discussion

Synthesis

Antimony(III) compounds were prepared via the lithium compounds obtained through the reaction of ether solutions of the corresponding amine the precursors with *n*-BuLi at 20°C to room temperature, followed by reaction with tritolylantimony and monobromodinitriles obtained from tribromides. The antimony(III) compounds thus obtained were further reacted with 1.2N sulfuryl chloride in CH₂Cl₂ to afford antimony(V) compounds (Scheme 1).

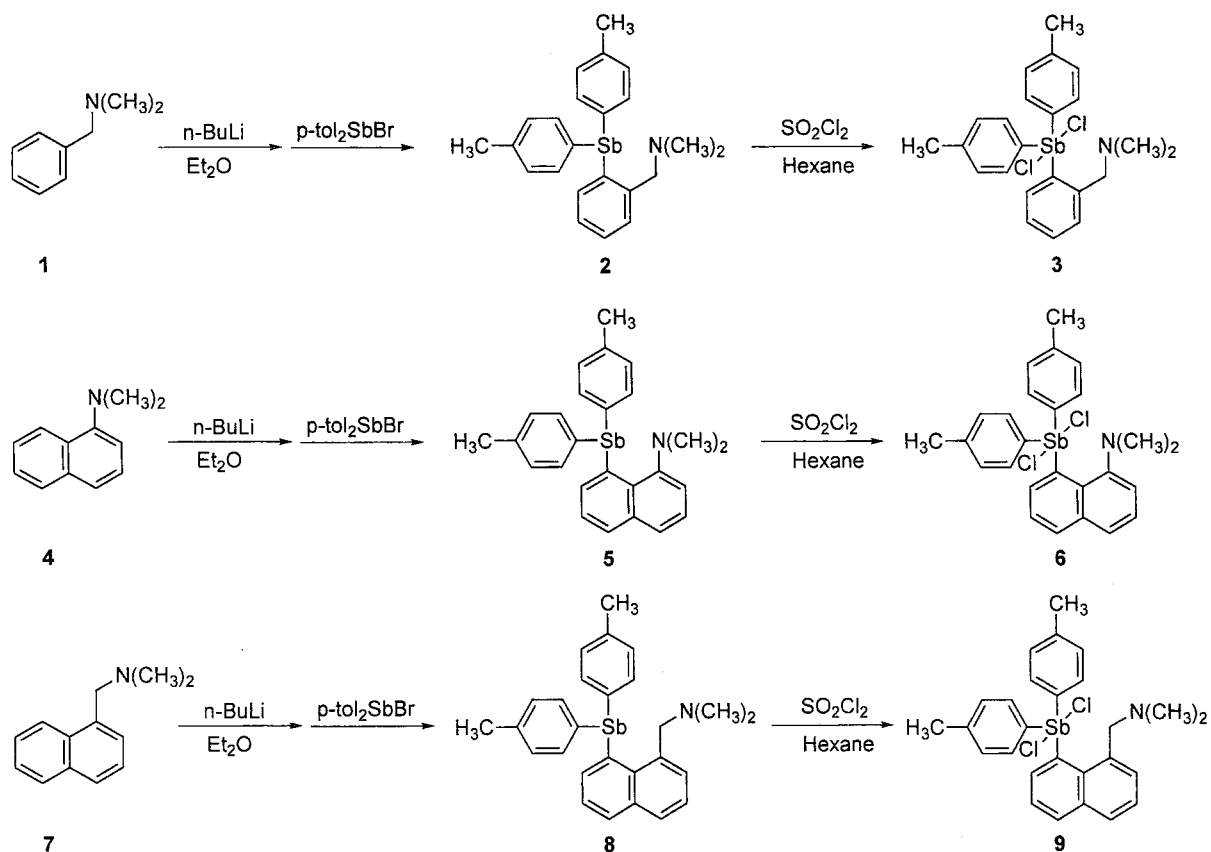
X-Ray analysis

X-Ray crystallographic analyses were undertaken to investigate the hypervalent Sb···N bonding in **2**, **3**, **5**, **6**, **8** and **9**. ORTEP drawings of the compounds are shown in Figs. 1–3. Bond lengths and angles are shown in Tables 1 and 2, respectively.

Observed Sb···N distances for these compounds were 69 to 77% of the sum of the van der Waals radii of 3.74 Å,¹³ suggesting the existence of strong inter atomic interaction.

Keywords: triarylstibane; X-ray crystallography; long-range coupling constant; ¹H–¹³C HMBC; ¹⁵N NMR; semi-empirical Hamiltonians.

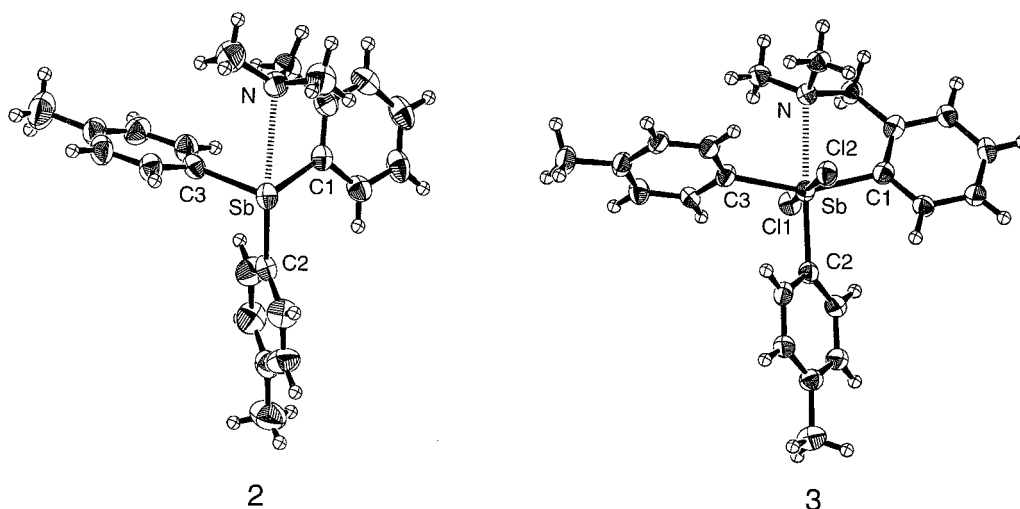
* Corresponding authors. Tel.: +81-43-290-3810; fax: +81-43-290-3813; e-mail: yamaguchi@cac.chiba-u.ac.jp



Scheme 1.

These distances are slightly longer than the covalent bond length of 2.11 Å.¹³ This result indicates hypervalent bond formation between antimony and nitrogen. In the case of compound **2**, the angles of N–Sb–C2, Cl–Sb–C2, C2–Sb–C3, and C3–Sb–C1 are 161.4(2), 93.5(3), 95.7(3) and 97.9(3)°, respectively, corresponding to a *pseudo*-trigonal-bipyramidal structure. The C2–Sb bond [2.162(6) Å] *trans* to the nitrogen atom is slightly longer than the other Sb–C bonds, 2.158(6) and 2.144(6) Å. This tendency, also observed in compounds **5** and **8**, is considered to be the hypervalent effect on the central antimony.

Antimony(V) exhibits further shortening (6 to 10%) of the Sb···N bond compared to antimony(III). This can be ascribed to the promotion of valence extension owing to increased Lewis acidity on the antimony caused by the introduction of two Cl atoms. In compound **3**, the N–Sb–C2 and Cl1(1)–Sb–Cl(2) angles, 172.9(2) and 175.3(5)°, respectively, are close to 180°, though Cl1–Sb–C3 is 156.6(2)°. The angles of Cl1–Sb–C3, Cl1–Sb–Cl(1), Cl1–Sb–Cl(2) and C3–Sb–Cl(2), involving the four atoms [Cl1, C3, Cl(1) and Cl(2)] equatorial to the N atom, are close to 90° (ranging from 86.7 to 92.6°). Moreover, the

Figure 1. ORTEP drawings of compounds **2** and **3**.

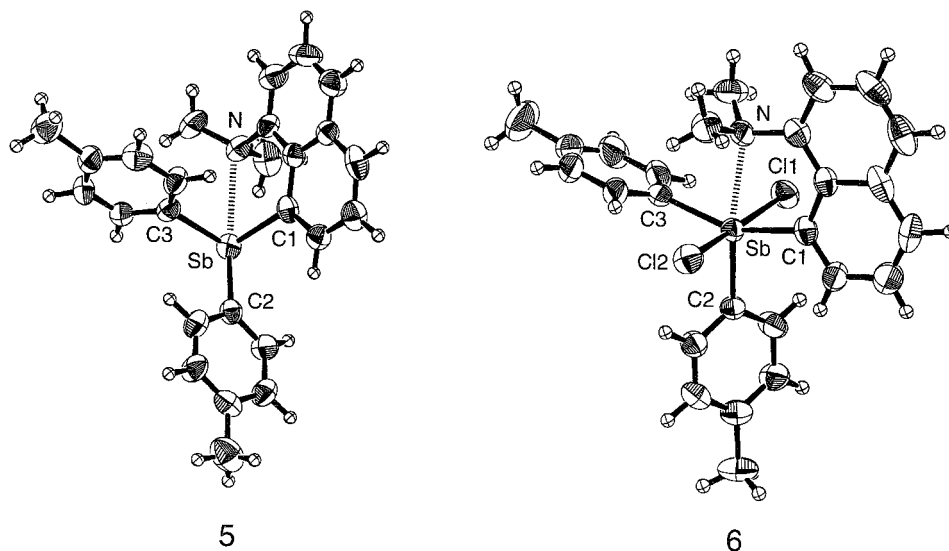


Figure 2. ORTEP drawings of compounds 5 and 6.

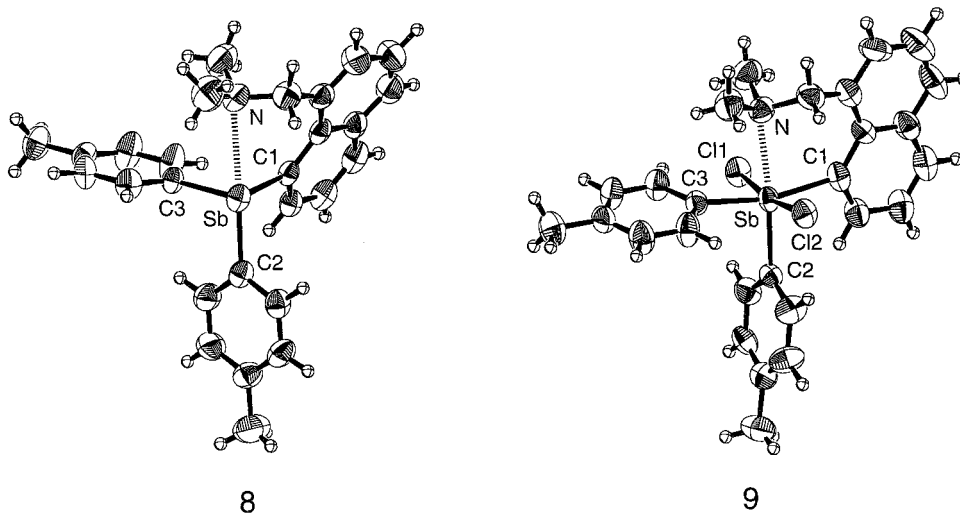


Figure 3. ORTEP drawings of compounds 8 and 9.

Table 1. Selected bond lengths (Å) and bond angles (°) for 2, 5, and 8

	2	5	8
Atomic distance (Å)			
Sb–N	2.874(6)	2.831(6)	2.766(4)
	3.74 ^a	3.74 ^a	3.74 ^a
	2.11 ^b	2.11 ^b	2.11 ^b
Sb–C1	2.158(6)	2.167(6)	2.190(4)
Sb–C2	2.162(6)	2.183(7)	2.184(5)
Sb–C3	2.144(6)	2.179(6)	2.154(4)
Bond angles (°)			
N–Sb–C2	161.4(3)	163.3(1)	172.3(1)
C1–Sb–C2	93.5(3)	95.6(2)	94.0(1)
C2–Sb–C3	95.7(3)	96.2(2)	95.2(1)
C3–Sb–C1	97.9(3)	96.9(2)	97.2(1)

^a Sum of the corresponding van der Waals radii.^b The corresponding covalent bond.

angles between C4 in the *trans* position and the equatorial atoms via Sb are 91.4 to 103.2°. It can be concluded from these results that compound 3 takes a *pseudo*-octahedral structure, consistent with hypervalent bond formation between antimony and nitrogen.

In a comparison of the two pairs of naphthalene compounds 5–8, and 6–9, the Sb···N distances of the compounds having a –CH₂N(CH₂)₂ group, which can form a 6-membered ring, are shorter than the others. This presumably reflects the flexible conformation that allows the nitrogen atom approach the central antimony, more closely.

No intermolecular short contact involving an antimony atom was observed in any crystal.

NMR analysis

Compounds 2, 5, and 8 exhibit *pseudo*-trigonal-bipyramidal

Table 2. Selected bond lengths (Å) and bond angles (°) for **3**, **6**, and **9**

	3	6	9
Atomic distance (Å)			
Sb–N	2.584(5)	2.658(4)	2.590(6)
	3.74 ^a	3.74 ^a	3.74 ^a
	2.11 ^b	2.11 ^b	2.11 ^b
Sb–C1	2.127(6)	2.141(5)	2.183(7)
Sb–C2	2.133(6)	2.129(5)	2.162(7)
Sb–C3	2.144(6)	2.160(5)	2.158(6)
Sb–Cl1	2.466(2)	2.492(1)	2.467(2)
Sb–Cl2	2.511(2)	2.473(1)	2.490(2)
Bond angles (°)			
N–Sb–C2	172.9(2)	174.7(1)	174.8(2)
C1–Sb–C3	156.5(2)	155.8(2)	166.3(3)
C11–Sb–Cl2	175.3(5)	172.3(5)	171.1(7)
C1–Sb–Cl1	89.0(1)	83.9(2)	85.0(2)
C11–Sb–C3	92.7(2)	92.5(2)	90.8(2)
C3–Sb–Cl2	90.4(2)	92.0(2)	92.1(2)
Cl2–Sb–C1	86.7(1)	89.4(2)	90.3(2)
C2–Sb–C1	103.2(2)	101.0(2)	100.7(3)
C2–Sb–C3	100.2(2)	103.1(2)	92.6(2)
C2–Sb–Cl1	91.4(1)	92.3(1)	95.5(2)
C2–Sb–Cl2	91.5(1)	92.8(1)	92.9(2)

^a Sum of the corresponding van der Waals radii.

^b The corresponding covalent bond.

structure in the crystal. However, the rotational energy barrier of the tolyl group is expected to be small in solution because equivalent ¹H NMR signals are observed for the two tolyl groups in each compound at 30°C. Therefore, these compound may take a distorted tetragonal structure with rapid equilibrium of the tolyl groups in solution.

On the other hand, a *pseudo*-octahedral structure of the dichloro compounds, **3**, **6**, and **9** was observed by means of X-ray crystallography. In the ¹H NMR spectrum at 30°C, the tolyl groups are not equivalent, and NOE (nuclear Overhauser effect) was observed between the *N*-methyl protons and one tolyl group. The tolyl group showing NOE with the *N*-methyl protons occupies the equatorial position and the other lies in the apical position. This strongly suggests that the antimony center has a *pseudo*-octahedral structure like that in the solid state in the cases of **3**, **6**, and **9**. A long-range coupling correlation between the *N*-methyl protons and the

Table 3. ¹⁵N NMR Chemical shifts and ⁴J_{(NCH₃-C₃) coupling constants observed for **1–9**}

Compound	¹⁵ N Chemical shift ^a δ _N =ppm	Coupling constant ^b ⁴ J _(NCH₃-C₃) =Hz
1	–353.6	
2	–350.7	2.3
3	–342.9	<0.5
4	–344.0	
5	–347.5	1.2
6	–343.2	1.6
7	–351.5	
8	–349.3	<0.5
9	–332.5	0.8

^a ¹⁵N NMR chemical shifts are referenced to neat CH₃NO₂ at 0 ppm as an external standard.

^b Coupling constants are absolute values obtained by *J*-HMBC 2D using selective excitation pulse.

quaternary carbons of the tolyl groups linked to the antimony atom was seen in a ¹H–¹³C HMBC (heteronuclear multiple bond correlation) experiment^{14,15} in compounds **2**, **3**, **5**, **6**, **8**, and **9**. Such a long-range coupling correlation through seven bonds seems highly improbable. It is more reasonable to interpret this coupling in terms of a four-bond correlation via Sb···N through Fermi-contact interaction,^{16,17} suggesting the presence of hypervalent bonding. The coupling constants between the *N*-methyl protons and the quaternary carbons of the tolyl group obtained by the *J*-HMBC 2D method^{18,19} are shown in Table 3. However, the coupling constants were all less than 2.3 Hz, and there seemed to be no clear relationship between coupling constants and the steric parameters such as bond length and angles.

The ¹⁵N chemical shifts of **2**, **3**, **5**, **6**, **8**, and **9** obtained by using ¹H–¹⁵N HMBC with natural abundance are also shown in Table 3. A low-field shift was seen in each compound. This might be caused by electron deficiency around the nitrogen atom owing to the delocalization of a pair of electrons, which would be consistent with Sb···N bonding.²⁰ However, a high-field shift, relative to **4**, was observed in **5**. This phenomenon can be explained as follows. A low-field shift is generally observed for aromatic amino-nitrogen based on the electron deficiency caused by withdrawal of the electron pair from the nitrogen to the aromatic ring. However, in the case of **5**, the electron transfer to the aromatic ring was restricted by the interaction with the central antimony. Attachment of the chlorine atoms to the antimony promotes Sb···N interaction because of increased Lewis acidity owing to the attached electro-negative elements; this result in the greater low-field shift observed in NMR. Furthermore, the Sb···N bonding distances of **3**, **6**, and **9** obtained from X-ray crystallography are shorter than those of **2**, **5**, and **8**. A correlation between Sb···N distances and ¹⁵N chemical shifts was also observed.

Theoretical calculations

The results of X-ray crystallography and NMR spectroscopy described above clearly demonstrate that the significant low-field shift observed in ¹⁵N NMR corresponds to shortening of the Sb···N bonding distance in the crystal structure. Semi-empirical molecular orbital calculations were performed to investigate the electronic character of this bonding.²¹ The calculations were carried out using the PM3-RHF (restricted Hartree-Fock) procedure²² (charge=0, multiplicity=1) with the standard parameters including the antimony atom as implemented in

Table 4. Molecular structure data of compounds **2**, **3**, **5**, **6**, **8** and **9** obtained by PM3 calculations

Compound	r(Sb–N) (Å)	Partial charge of nitrogen ^a	∠N–Sb–C2 (°)
2	2.749	–0.0546	164.5
3	2.649	–0.0211	172.4
5	2.625	0.0117	166.2
6	2.658	0.0379	176.0
8	2.659	–0.0484	173.6
9	2.552	0.0090	174.5

^a Partial charges of nitrogen are given in the au unit.

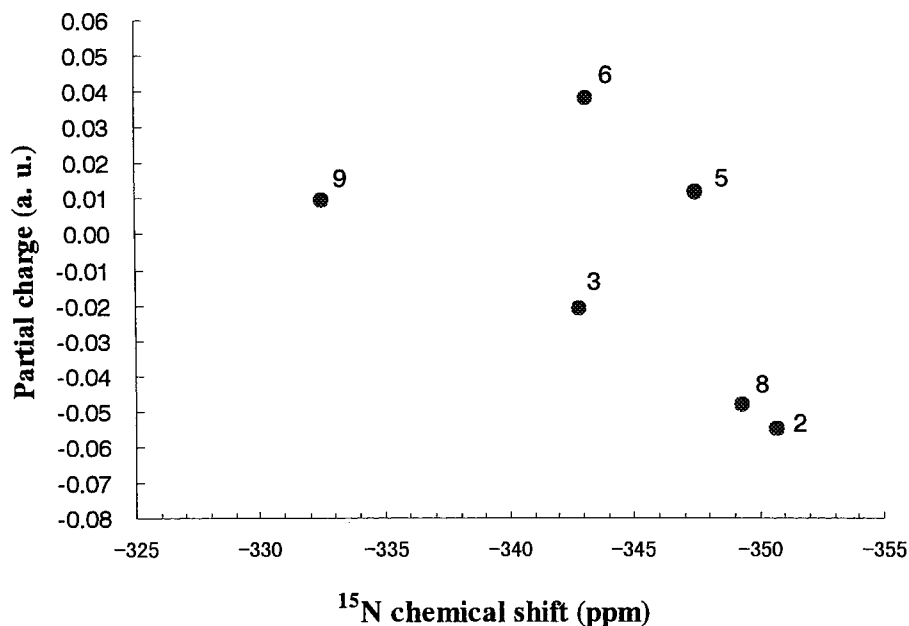


Figure 4. Correlation of ¹⁵N chemical shifts with partial charges calculated by using the PM3 method.

MOPAC.²³ The geometry of the compounds was obtained by minimizing the total energy using the Polak–Ribiere optimization procedure starting from the coordinates obtained from X-ray crystallography.

As shown in Table 4, the existence of hypervalent Sb···N bonding is also confirmed by these calculations because almost identical values of bond lengths and dihedral angles involving the antimony atom, were obtained, compared to those obtained from X-ray analyses. The correlation of the chemical shifts of ¹⁵N with the calculated electron densities is shown in Fig. 4.

The correlation between these parameters was high for **2**, **3**, **8**, and **9**, in which the amino group is not connected directly to the aromatic ring. The charge distribution on the nitrogen is an important parameter^{24–27} to estimate the bonding nature of the connected atoms in this class of compounds.

Conclusion

The existence of strong interactions between antimony and nitrogen, transcending the octet theory, and classified as the hypervalent bonding, was proved not only in cyclic antimony compounds but also in the acyclic ones. This hypervalent Sb···N bonding was demonstrated by single-crystal X-ray analyses, comparison of the ¹⁵N chemical shifts and detection of the ¹H–¹³C long-range coupling by HMBC NMR measurements. It was also confirmed that the interaction strongly depends on the Lewis acidity of the central antimony atom. A good correlation was observed between ¹⁵N chemical shifts and the charge distributions calculated by the semi-empirical method. The value of the ¹⁵N chemical shift appears to reflect well the status of the Sb···N bonding.

Experimental

General procedures

All melting points were measured on a Yanaco micro melting point hot stage apparatus and are uncorrected. Mass spectra were recorded on a JEOL JMS-SX102A instrument (EI, 10 kV Accel.). Elemental analyses were determined on a Yanaco MT-5 CHN coder. ¹H and ¹⁵N NMR spectra were recorded on a JEOL JNM-LA600 spectrometer in CD₂Cl₂ at 303 K. ¹⁵N Chemical shifts were obtained from cross peaks of ¹H–¹⁵N HMBC spectra. Chemical shifts are given in δ values (ppm) referenced to the proton of CD₂Cl₂, as an internal standard (5.32 ppm) for ¹H and neat nitromethane as an external standard (0 ppm) for ¹⁵N.

General procedure for the synthesis of triarylstibanes (**2**, **5**, and **8**)

To a solution of the amine (15 mmol) in ether (20 mL) was added butyllithium (1.6 M in hexane, 12 mL, 18 mmol) at 0°C under an argon atmosphere, and the solution was stirred for 24 h at room temperature. To this was added a solution of bromobis(4-methylphenyl)stibine [prepared via a redistribution reaction by heating tris(4-methylphenyl)stibane (3.15 g, 8 mmol) and tribromostibane (1.6 g: 90%, 4 mmol) for 1 h at 90°C] in ether (30 mL) over 15 min at 0°C, and the mixture was stirred for 1–3 h at the same temperature. The mixture was quenched with water (50 mL) and diluted with benzene (50 mL), and insoluble polymeric substances were removed by filtration. The organic layer was separated and the aqueous layer was extracted with benzene (50 mL). The combined organic layer was washed with brine, dried, and evaporated in vacuo. The resulting product was purified by passage through a short column of aluminum oxide using hexane for **2** or hexane/dichloromethane (5:1) mixture for **5** and **8** as an eluent, to furnish the triarylstibane.

2-(*N,N*-Dimethylaminomethyl)phenylbis(4-methylphenyl)-stibane (2). Yield 3.80 g (58%), colorless prisms, mp 88–89°C from methanol–dichloromethane; $^1\text{H NMR}$ (CD_2Cl_2) 1.89 (s, 6H), 2.33 (s, 6H), 3.45 (s, 2H), 7.11–7.13 (m, 5H), 7.16 (d, 1H, $J=7.3$ Hz), 7.24 (t, 1H, $J=7.3$ Hz), 7.26 (d, 1H, $J=7.3$ Hz), 7.33 (d, 4H, $J=7.3$ Hz); MS m/z : 437 (M^+). Anal. Calcd for $\text{C}_{23}\text{H}_{26}\text{NSb}$: C, 63.04; H, 5.98; N, 3.20. Found: C, 63.30; H, 5.93; N, 3.26.

1-[8-(*N,N*-Dimethylamino)naphthyl]bis(4-methylphenyl)-stibane (5). Yield 2.77 g (39%), colorless prisms, mp 174–176°C from benzene; $^1\text{H NMR}$ (CD_2Cl_2) 2.29 (s, 6H), 2.42 (s, 6H), 7.04 (d, 4H, $J=7.7$ Hz), 7.15 (d, 4H, $J=7.7$ Hz), 7.32 (m, 2H), 7.37 (d, 1H, $J=7.0$ Hz), 7.46 (t, 1H, $J=8.3$ Hz), 7.73 (d, 1H, $J=8.3$ Hz), 7.84 (d, 1H, $J=8.1$ Hz); MS m/z : 473 (M^+). Anal. Calcd for $\text{C}_{26}\text{H}_{26}\text{NSb}$: C, 65.85; H, 5.53; N, 2.95. Found: C, 65.90; H, 5.59; N, 2.91.

1-[8-(*N,N*-Dimethylaminomethyl)naphthyl]bis(4-methylphenyl)stibane (8). Yield 3.29 g (45%), colorless prisms, mp 148–150°C from methanol–dichloromethane; $^1\text{H NMR}$ (CD_2Cl_2) 1.79 (s, 6H), 2.33 (s, 6H), 4.17 (s, 2H), 7.10 (d, 4H, $J=8.1$ Hz), 7.27 (t, 1H, $J=7.0$ Hz), 7.29 (d, 4H, $J=8.1$ Hz), 7.36–7.42 (m, 2H), 7.82 (d, 1H, $J=7.0$ Hz), 7.83 (m, 2H); MS m/z : 487 (M^+). Anal. Calcd for $\text{C}_{27}\text{H}_{28}\text{NSb}$: C, 66.42; H, 5.78; N, 2.87. Found: C, 66.25; H, 5.85; N, 2.95.

General procedure for the synthesis of dichlorotriaryl- λ^5 -stibanes (3, 6, and 9)

A solution of SO_2Cl_2 (160 mg, 1.2 mmol) in hexane (2 mL) was added to a stirred solution of arylbis(4-methylphenyl)-stibane (1.0 mmol) in dichloromethane (5 mL) under cooling with an ice bath, and the mixture was stirred for 30 min at 0°C. The mixture was evaporated in vacuo, and the resulting residue was recrystallized from acetonitrile to afford the λ^5 -stibane.

Dichloro[2-(*N,N*-dimethylaminomethyl)phenyl]bis(4-methylphenyl)- λ^5 -stibane (3). Yield 343 mg (63%), colorless prisms, mp 205–207°C from acetonitrile; $^1\text{H NMR}$ (CD_2Cl_2) 2.20 (s, 6H), 2.39 (s, 3H), 2.41 (s, 3H), 3.89 (s, 2H), 7.26 (m, 3H), 7.31–7.36 (m, 3H), 7.43 (t, 1H, $J=7.3$ Hz), 7.49 (d, 1H, $J=7.3$ Hz), 7.78 (d, 2H, $J=8.0$ Hz), 8.26 (d, 2H, $J=8.0$ Hz); MS m/z : 472 ($\text{M}^+ - \text{Cl}$). Anal. Calcd for $\text{C}_{23}\text{H}_{26}\text{Cl}_2\text{NSb}$: C, 52.58; H, 4.99; N, 2.67. Found: C, 52.57; H, 4.92; N, 2.63.

Dichloro-1-[8-(*N,N*-dimethylamino)naphthyl]bis(4-methylphenyl)- λ^5 -stibane (6). Yield 343 mg (63%), colorless prisms, mp 243–246°C from acetonitrile; $^1\text{H NMR}$ (CD_2Cl_2) 2.38 (s, 3H), 2.43 (s, 3H), 2.61 (s, 6H), 7.26 (d, 2H, $J=8.0$ Hz), 7.38 (d, 2H, $J=8.0$ Hz), 7.55 (m, 2H), 7.60 (t, 1H, $J=8.0$ Hz), 7.71 (d, 1H, $J=7.0$ Hz), 7.84 (d, 1H, $J=8.0$ Hz), 7.91 (d, 2H, $J=8.0$ Hz), 7.98 (d, 1H, $J=8.0$ Hz); MS m/z : 508 ($\text{M}^+ - \text{Cl}$). Anal. Calcd for $\text{C}_{26}\text{H}_{26}\text{Cl}_2\text{NSb}$: C, 57.28; H, 4.81; N, 2.57. Found: C, 57.35; H, 4.74; N, 2.62.

Dichloro-1-[8-(*N,N*-dimethylaminomethyl)naphthyl]bis(4-methylphenyl)- λ^5 -stibane (9). Yield 379 mg (68%), colorless prisms, mp 203–204°C from acetonitrile; $^1\text{H NMR}$

(CD_2Cl_2) 2.17 (s, 6H), 2.34 (s, 3H), 2.36 (s, 3H), 4.70 (brs, 2H), 7.16 (d, 2H, $J=8.0$ Hz), 7.26 (d, 2H, $J=8.0$ Hz), 7.36 (t, 1H, $J=7.7$ Hz), 7.38 (d, 1H, $J=8.0$ Hz), 7.48 (t, 1H, $J=8.0$ Hz), 7.80 (d, 2H, $J=8.0$ Hz), 7.86 (d, 1H, $J=7.7$ Hz), 7.89 (d, 1H, $J=8.0$ Hz), 7.92 (d, 1H, $J=8.0$ Hz), 8.35 (d, 2H, $J=8.0$ Hz); MS m/z : 522 ($\text{M}^+ - \text{Cl}$). Anal. Calcd for $\text{C}_{27}\text{H}_{28}\text{Cl}_2\text{NSb}$: C, 58.16; H, 5.07; N, 2.51. Found: C, 58.32; H, 5.06; N, 2.61.

X-Ray studies

A Rigaku AFC7S diffractometer employing graphite-monochromated Cu K_α radiation or a RAXIS-II diffractometer with graphite-monochromated Mo K_α radiation was used.

All calculations were performed using the teXsan crystal structure solution software package.²⁸

Crystallographic data for 2.²⁹ $\text{C}_{23}\text{H}_{26}\text{NSb}$, $M=438.22$, triclinic, space group $\text{P}\bar{1}$ (#2), $a=11.0727(9)$, $b=20.111(1)$, $c=10.0956(8)$ Å, $\alpha=104.358(6)$, $\beta=105.936(6)$, $\gamma=80.861(6)^\circ$, $V=2084.3(3)$ Å³, $Z=4$, $D_{\text{calc}}=1.396$ g cm⁻³, $T=296.2$ K, $\mu=10.48$ cm⁻¹ (Cu $\text{K}_\alpha=1.5418$ Å), $R=0.047$ ($R_w=0.054$) for 5855 observed reflections [$I>2.0\sigma(I)$], GOF=1.808 (452 parameters).

Crystallographic data for 3. $\text{C}_{23}\text{H}_{26}\text{NCl}_2\text{Sb}$, $M=509.12$, monoclinic, space group $\text{P}2_1/\text{n}$ (#14), $a=14.689(9)$, $b=9.90(1)$, $c=16.47(1)$ Å, $\beta=113.35(1)^\circ$, $V=2200.6699(3)$ Å³, $Z=4$, $D_{\text{calc}}=1.537$ g cm⁻³, $T=296.2$ K, $\mu=15.02$ cm⁻¹ (Mo $\text{K}_\alpha=0.7107$ Å), $R=0.050$ ($R_w=0.068$) for 3396 observed reflections [$I>2.0\sigma(I)$], GOF=1.994 (244 parameters).

Crystallographic data for 5. $\text{C}_{26}\text{H}_{26}\text{NSb}$, $M=474.25$, monoclinic, space group $\text{P}2_1/\text{n}$ (#14), $a=10.1613(12)$, $b=16.081(2)$, $c=13.607(2)$ Å, $\beta=98.190(2)^\circ$, $V=2200.7(4)$ Å³, $Z=4$, $D_{\text{calc}}=1.431$ g cm⁻³, $T=299.2$ K, $\mu=12.62$ cm⁻¹ (Mo $\text{K}_\alpha=0.7107$ Å), $R=0.046$ ($R_w=0.047$) for 2921 observed reflections [$I>2.0\sigma(I)$], GOF=1.910 (254 parameters).

Crystallographic data for 6. $\text{C}_{26}\text{H}_{26}\text{NCl}_2\text{Sb}$, $M=545.15$, monoclinic, space group $\text{P}2_1/\text{n}$ (#14), $a=10.6866(12)$, $b=12.100(1)$, $c=18.797(1)$ Å, $\beta=99.396(3)^\circ$, $V=2398.0(4)$ Å³, $Z=4$, $D_{\text{calc}}=1.510$ g cm⁻³, $T=298.2$ K, $\mu=13.84$ cm⁻¹ (Mo $\text{K}_\alpha=0.7107$ Å), $R=0.038$ ($R_w=0.041$) for 9654 observed reflections [$I>2.0\sigma(I)$], GOF=1.720 (272 parameters).

Crystallographic data for 8. $\text{C}_{27}\text{H}_{28}\text{NSb}$, $M=488.27$, monoclinic, space group $\text{P}2_1/\text{n}$ (#14), $a=10.1119(12)$, $b=14.415(2)$, $c=15.995(3)$ Å, $\beta=95.233(2)^\circ$, $V=2321.7(5)$ Å³, $Z=4$, $D_{\text{calc}}=1.397$ g cm⁻³, $T=299.2$ K, $\mu=11.99$ cm⁻¹ (Mo $\text{K}_\alpha=0.7107$ Å), $R=0.039$ ($R_w=0.036$) for 3074 observed reflections [$I>2.0\sigma(I)$], GOF=1.320 (263 parameters).

Crystallographic data for 9. $\text{C}_{27}\text{H}_{28}\text{NCl}_2\text{Sb}$, $M=559.18$, monoclinic, space group $\text{P}2_1/\text{c}$ (#14), $a=17.327(3)$, $b=9.0509(6)$, $c=17.399(6)$ Å, $\beta=113.35(1)^\circ$, $V=2414(1)$ Å³, $Z=4$, $D_{\text{calc}}=1.538$ g cm⁻³, $T=296.2$ K, $\mu=11.17$ cm⁻¹ (Cu $\text{K}_\alpha=1.5418$ Å), $R=0.039$ ($R_w=0.045$)

for 2771 observed reflections [$I > 2.0\sigma(I)$], GOF=1.225 (281 parameters).

References

1. David, A.; Cowley, A. H.; Ruiz, J. *Inorg. Chim. Acta* **1992**, *198–200*, 271–274.
2. Suzuki, H.; Murafuji, T.; Matano, Y.; Azuma, N. *J. Chem. Soc., Perkin Trans. 1* **1993**, 2969–2973.
3. Murafuji, T.; Mutoh, T.; Satoh, K.; Tsunenari, K.; Azuma, N.; Suzuki, H. *Organometallics* **1995**, *14*, 3848–3854.
4. Iwaoka, M.; Tomoda, S. *J. Org. Chem.* **1995**, *60*, 5299–5302.
5. Iwaoka, M.; Tomoda, S. *J. Am. Chem. Soc.* **1996**, *118*, 8077–8084.
6. Chuit, C.; Corriu, R. J. P.; Monforte, P.; Reyé, C.; Declercq, J. P.; Dubourg, A. *J. Organomet. Chem.* **1996**, *511*, 171–175.
7. Carmalt, C. J.; Cowley, A. H.; Culp, R. D.; Jones, R. A.; Kamepalli, S.; Norman, N. C. *Inorg. Chem.* **1997**, *36*, 2770–2776.
8. Yamamoto, Y.; Chen, X.; Kojima, S.; Ohdoi, K.; Kitano, M.; Doi, Y.; Akiba, K. *J. Am. Chem. Soc.* **1995**, *117*, 3922–3932.
9. Yasuike, S.; Tsukada, S.; Kurita, J.; Tsuchiya, T.; Tsuda, Y.; Kikuchi, H.; Hosoi, S. *Heterocycles* **2000**, *53*, 525–528.
10. Ohtaka, K.; Takemoto, S.; Ohnishi, M.; Akiba, K. *Tetrahedron Lett.* **1989**, 4841–4844.
11. Yamamoto, Y.; Chen, X.; Akiba, K. *J. Am. Chem. Soc.* **1992**, *114*, 7906–7907.
12. Minoura, M.; Kanamori, Y.; Miyake, A.; Akiba, K. *Chem. Lett.* **1999**, 861–862.
13. Emsley, J. *The Elements*, 3rd edition, Clarendon: Oxford, 1998.
14. Bax, A.; Summers, M. F. *J. Am. Chem. Soc.* **1986**, *108*, 2093–2094.
15. Hurd, R. E.; John, B. K. *J. Magn. Reson.* **1991**, *91*, 648–653.
16. Ramsey, N. F.; Purcell, E. M. *Phys. Rev.* **1952**, *85*, 143–144.
17. Abraham, R. J.; Loftus, P. *Proton and Carbon-13 NMR Spectroscopy*, Heyden: London, 1978.
18. Willker, W.; Leibfritz, D. *Magn. Reson. Chem.* **1995**, *33*, 632–638.
19. Seki, H.; Tokunaga, T.; Utsumi, H.; Yamaguchi, K. *Tetrahedron* **2000**, *56*, 2935–2939.
20. Levy, G. C.; Lichter, R. L. *Nitrogen-15 NMR Spectroscopy*, Wiley: New York, 1979.
21. All PM3 calculations were carried out using the HYPERCHEM ver. 5.01 program system with a Faith INSPIRE-600BX/EJ personal computer.
22. Stewart, J. J. P. *J. Comput. Chem.* **1989**, *10*, 209–2120.
23. Stewart, J. J. P. *QCPE*, #454.
24. Matsumoto, K.; Ciobanu, M.; Uchida, T.; Machiguchi, T. *Heterocycles* **1997**, *46*, 645–650.
25. Matsumoto, K.; Katsura, H.; Uchida, T.; Aoyama, K.; Machiguchi, T. *Heterocycles* **1997**, *45*, 2443–2448.
26. Kolehmainen, E.; Saman, D.; Pískala, A.; Masojídková, M. *Mag. Res. Chem.* **1995**, *33*, 690–693.
27. Kolehmainen, E.; Tamminen, J.; Kauppinen, R.; Linnanto, J. *J. Inclusion Phenom. Macrocyclic Chem.* **1999**, *35*, 75–84.
28. Crystallographic data for the new structures reported in this paper have been deposited with the Cambridge Crystallographic Data Center. The coordinates can be obtained, on request, from the Director, Cambridge Crystallographic Data Center, 12 Union Road, Cambridge, CB2 1EZ, UK. Ref. No. for **2** CCDC 149376, for **3** CCDC 149377, for **5** CCDC 149378, for **6** CCDC 149379, for **8** CCDC 149380 and for **9** CCDC 149381.
29. Two independent molecules are contained in an asymmetric unit in the crystal. The geometrical parameters of **2** given in the text are averaged.